Supplementary Information

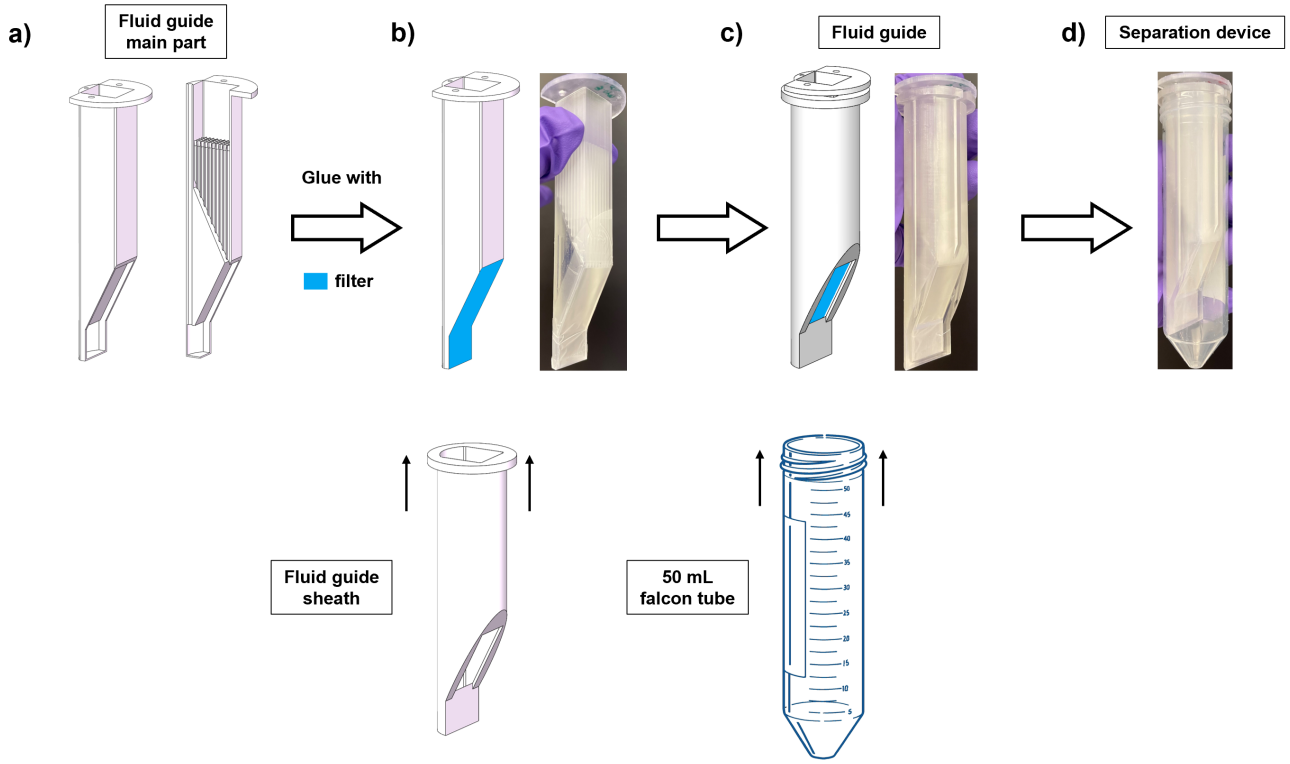

Figure 1: **Schematics and photographs of the fluid guide and its assembly.** a) CAD image of the fluid guide main part with a section view. b) Integration of the filter (blue) into the fluid guide by sliding the fluid guide sheath over the filter and fluid guide main part. c) Mounting of the fluid guide into a centrifuge tube. d) The complete separation device.

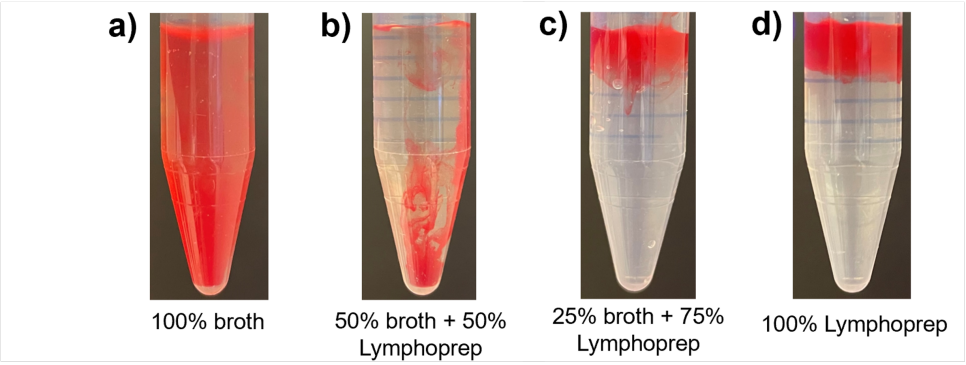

Figure 2: **Photographs of whole blood loaded on media with different densities:** a) 100% broth, b) 50% broth + 50% Lymphoprep, c) 25% broth + 75% Lymphoprep, and d) 100% Lymphoprep.

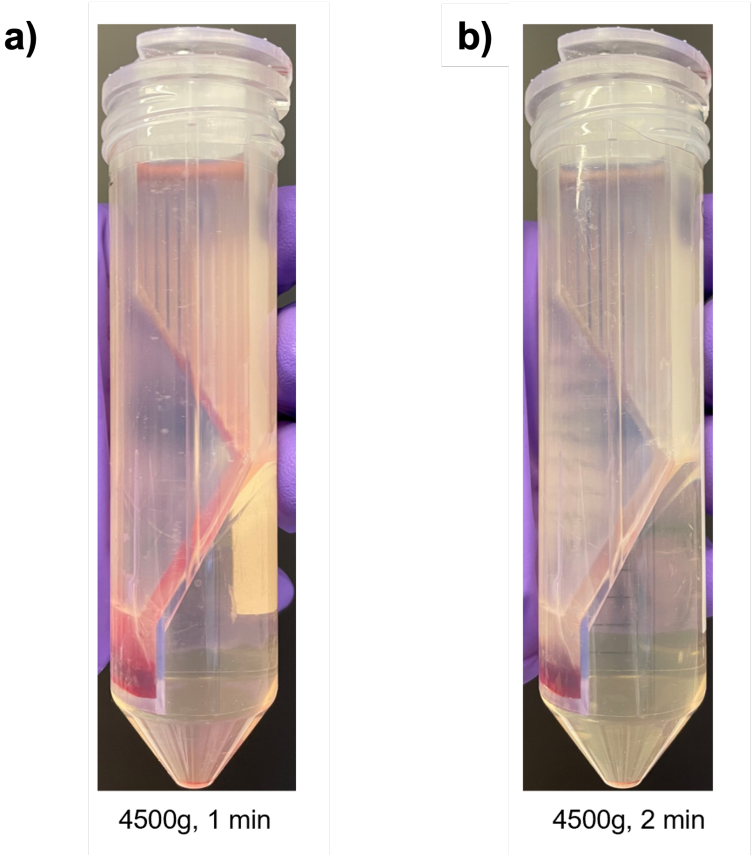

Figure 3: **Photographs of the device after a) one and b) two min centrifugation.**

Coriolis mixing

During device development, we observed Coriolis mixing to convectively mix the sample during centrifugal acceleration and deceleration. We studied this phenomenon by integrating a wireless camera (Global Tsolar Lights Electrical, China) and light source (Ledlenser, Germany) next to a centrifuge tube during centrifuge operation (Figure 4). The holder used for filming inside the centrifuge is shown in (Figure S5†) and contains pockets for the camera, light source and fluidic device. During centrifuging, the camera sends images of the centrifugation wirelessly from within the centrifuge to a computer outside the centrifuge. Despite the suboptimal image quality in this cramped optical configuration, the obtained results were sufficient for visual inspection of the centrifugation process. We compared centrifuge tubes with and without vertical grid structures. The centrifuge was accelerated to 10000 g and visualized continuously in real-time. In centrifuge tubes without a grid, the blood was convectively mixed with the density medium within seconds. In contrast, in centrifuge tubes with a grid, most blood cells moved by sedimentation rather than convection. We conclude that the grid efficiently reduced the mixing by blocking horizontal flow components. We made an attempt to recover bacteria from the separation device without the grid structure and received fewer bacteria recovery (around 26%).

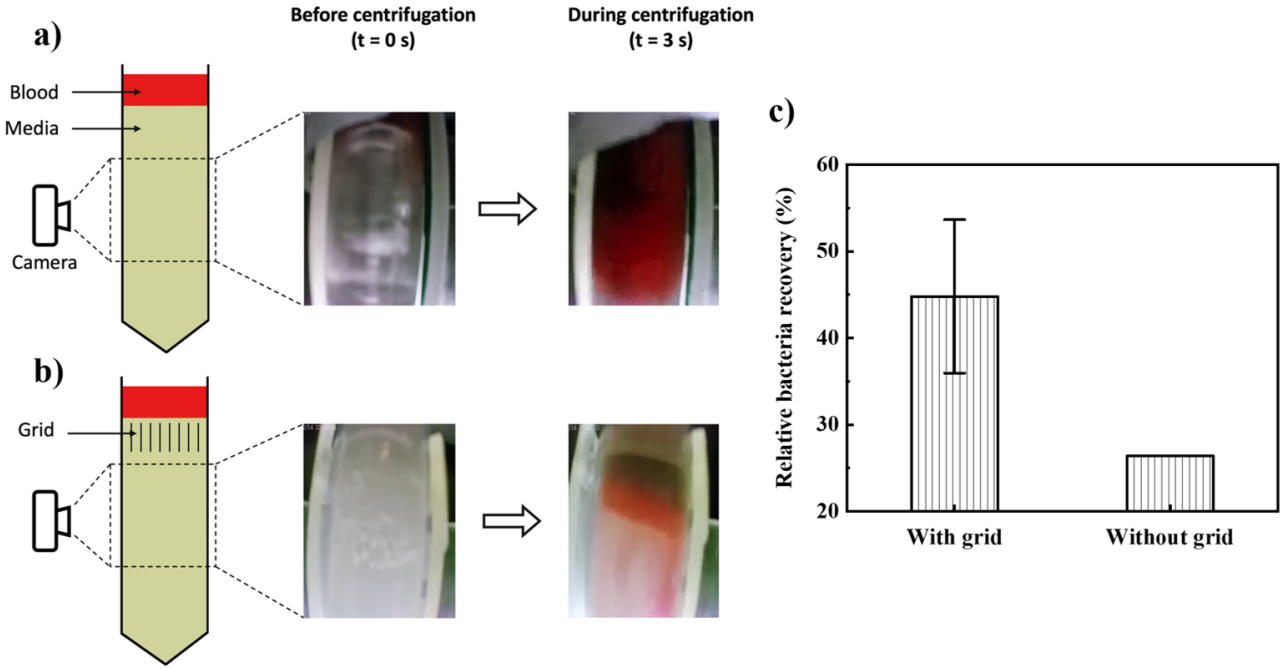

Figure 4: **The effect of grid structures on Coriolis mixing during centrifugal acceleration.** Schematic (left) and side-view photographs of density medium in a centrifuge tube after loading of blood (middle) and 3 s after the onset of centrifugation (right) for structures without (a) and with (b) a grid. (c) Relative bacteria recovery from the separation device with and without the grid structure. Results are for 10^4 CFU/mL of *K. pneumoniae* spiked in 0.4 mL of whole blood, using 75% Lymphoprep + 25% broth medium, 63 °filter angle, 3.0 µm pore size filter, and centrifuging for 30 min at 4500g.

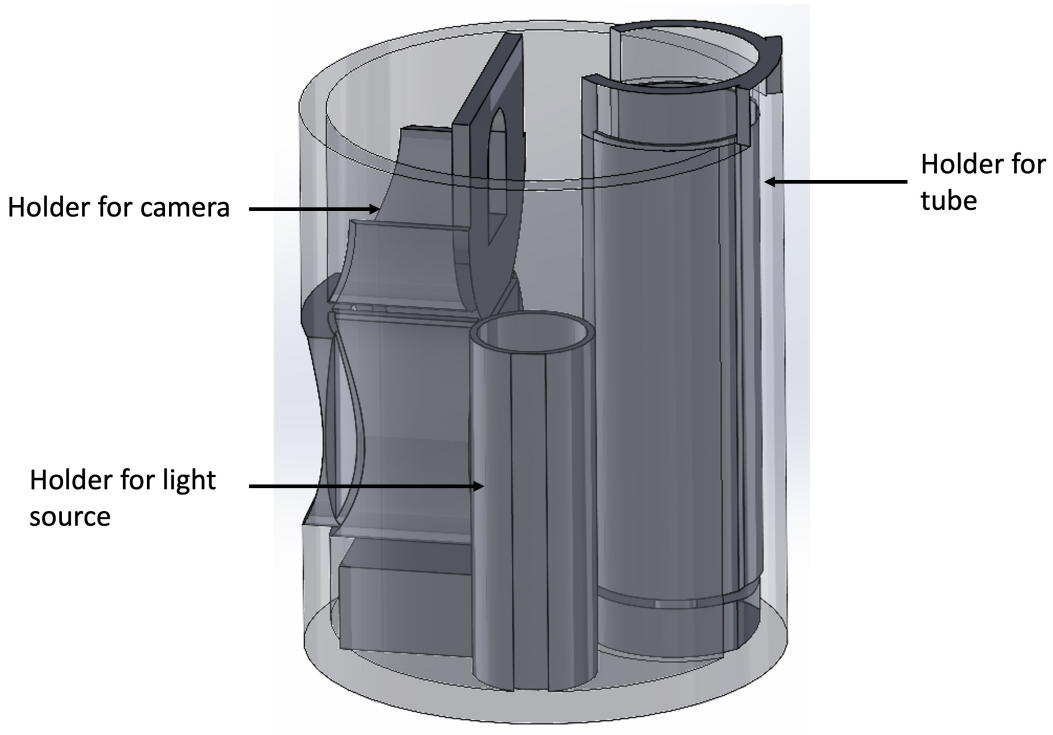

Figure 5: **The design of the centrifuge holder for capturing the video inside the centrifuge. The centrifuge holder consists of a holder for a tube, camera and light source, which was placed inside the centrifuge to visualize the mixing of the blood.**

Bacterial interaction with the surface of 3D-printed structures

To investigate the interaction of bacteria with the rough surface of 3D-printed structures, we compared bacterial recovery from 3D-printed tubes with that from commercial centrifuge tubes (injection molded in polypropylene). We 3D-printed centrifuge tubes with the same geometry as the commercial tubes, added 2 mL of medium of 75% Lymphoprep + 25% broth, spiked with 1000 CFU/ml *E. coli*. After centrifugation for 30 min at 4500g, we quantitated the bacteria in the tube by plate culture. From the commercial tube, we recovered $1.7e3 \pm 0.3e3$ CFU (sd, n=3), whereas this number was $1.0e3 \pm 0.2e3$ (sd, n=3) (Figure 6). The bacteria loss can thus be estimated to be (1 - [CFU commercial/CFU 3D-printed]) is thus $4e1 \pm 1e1\%$ (68% CI).

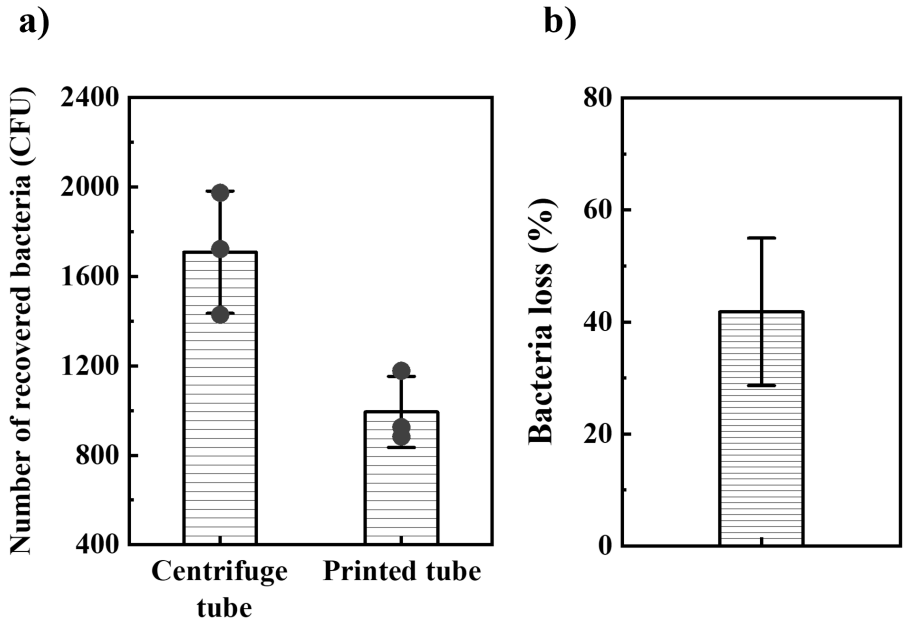

Figure 6: **Bacterial recovery from commercial and 3D printed centrifuge tubes.**

Determination of RBC fractions

We determined the relative RBC fraction in the filtrate and retentate as follows. We performed our centrifugation protocol on samples of donor blood without bacteria. We performed a series of dilutions of aliquots of filtrate and retentate in DIW and measured the light absorbance by hemoglobin (Figure 7). We measured the slope of the linear range of the measurements and compared those between filtrate and retentate to determine the relative RBC fraction. For the retentate samples, concentrations over 20% clearly deviate from a linear range. To avoid using the non-linear data points, we took the concentrations ranging from 0% to 10% for the slope calculation. In the filtrate samples, RBC concentration is much less than in the retentate sample. Therefore, concentrations ranging from 0% to 100% are taken for the slope calculation, as they easily manifest a linear relationship in the graphs.

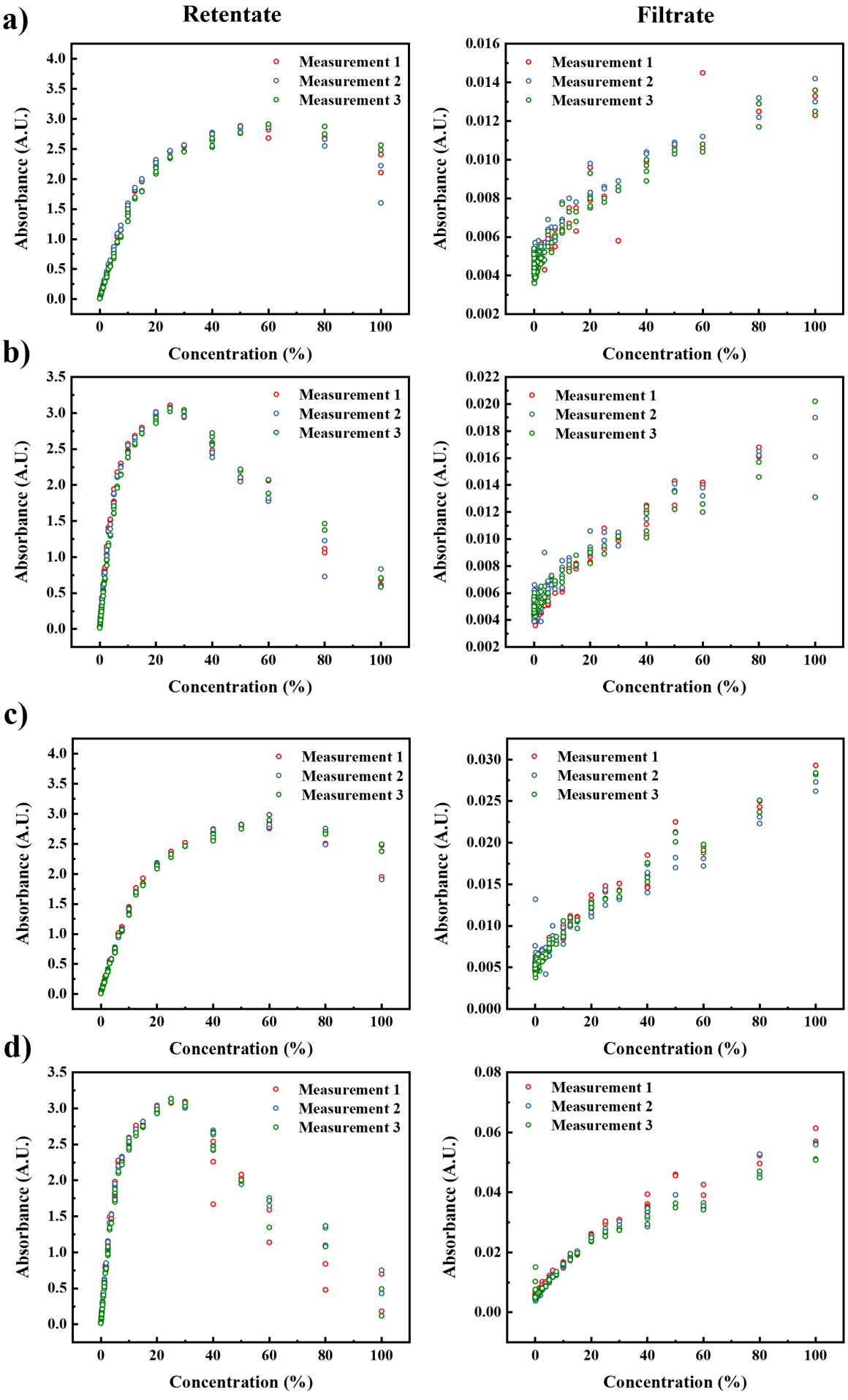

Figure 7: **Light absorbance by Hb for different mixtures of retentate or filtrate sample and DIW.** Measurement 1, 2, and 3 refers to three different experiments performed with the blood of the same donor. Concentration means the volume of sample/total volume. The filter pore size and blood volume were, respectively, a) 2.0 µm and 0.4 mL, b) 2.0 µm and 1.0 mL, c) 3.0 µm and 0.4 mL, and d) 3.0 µm and 1.0 mL.

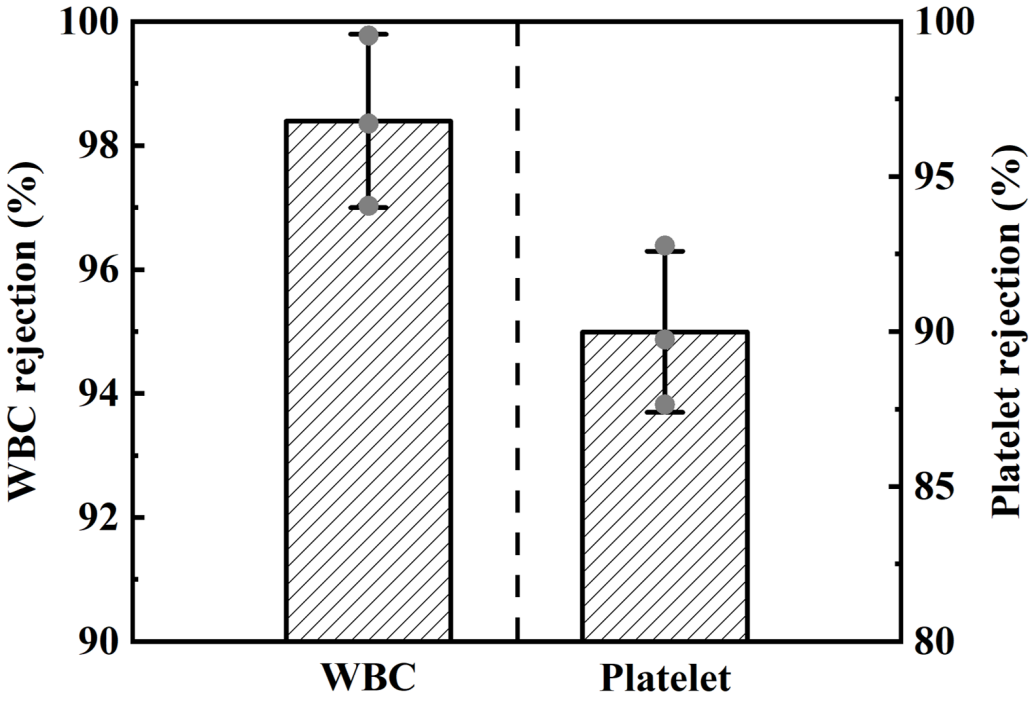

Figure 8: **WBC and platelet rejection for a filter with 3.0 m pore size and 1 mL blood sample volume. Error bars are sd.**